Inorg. Chem. **2008**, *47*, 1346−1351

Porous Metal−Organic Framework Based on μ_4-oxo Tetrazinc Clusters: Sorption and Guest-Dependent Luminescent Properties

Lei Hou, **Yan-Yong Lin**, **and Xiao-Ming Chen***

MOE Key Laboratory of Bioinorganic and Synthetic Chemistry, School of Chemistry and Chemical Engineering, Sun Yat-Sen University, Guangzhou 510275, China

Received October 22, 2007

A three-dimensional, highly porous metal−organic framework $[Zn_4O(bdc)(bpz)_2]\cdot 4DMF\cdot 6H_2O$ (**1**) (bdc = 1,4-benzenedicarboxylate, bpz = 3,3′,5,5′-tetramethyl-4,4′-bipyrazolate) constructed by Zn_4O clusters with bdc and bpz linkers, has been prepared and structurally characterized. The N_2 sorption measurements reveal that **1** exhibits high porosity with a Langmuir surface area of 1908 m^2/g and a pore volume of 0.58 cm^3/g. Compound **1** features hydrophobic channels with a free passage of ∼8.2 Å defined by the methyl groups from bpz, and it exhibits nice sorption capability for benzene and toluene and interesting two-step sorption behavior for methanol. Meanwhile, **1** also exhibits interesting guest-dependent luminescent properties.

Introduction

Porous metal−organic frameworks (MOFs) are a hot topic because of their promising applications in separation,[1] molecular storage,[2] molecular magnets,[3] and semiconductors.[4] For functionality, many types of organic ligands and metal motifs, such as dinuclear, trinuclear, tetranuclear, and even higher-nuclear clusters have been used as SBUs to construct robust and highly porous MOFs.[1a,3b,5] In particular, the tetrahedral Zn_4O clusters have been successfully incorporated into MOFs with multitopic carboxylate linkers, and many of them are of high thermal stability, have high guest adsorption capacity, and are promising for industrial applications.[6] Zn_4O clusters, being of a medium size, can serve as vertexes to furnish open MOFs and prevent interpenetration of the frameworks to attain high porosity. However, most organic ligands in such type of MOFs are polytopic arylcarboxylate,[6a,7] while azolates, such as pyrazolates, imidazolates, triazolates, and tetraazolates, have not been reported to connect such M_4O clusters into analogous MOFs according to the latest Cambridge Crystallographic Database (CCD, version 5.28).

It is already known that 3,3′,5,5′-tetramethyl-4,4′-bipyrazolate (bpz) (Scheme 1) can act as a neutral bridging ligand by using both pyrazole ends to ligate a pair of divalent metal ions, and more interestingly, it can also serve as anionic, tetradentate ligand to bridge four metal ions, such as Cu(II),

* To whom correspondence should be addressed. Fax: (86)-20-84112245. Phone: (86)-20-84113986. E-mail: cxm@mail.sysu.edu.cn.

(1) (a) Ma, S.; Sun, D.; Wang, X.-S.; Zhou, H.-C. *Angew. Chem., Int. Ed.* **2007**, *46*, 2458. (b) Chen, B.; Liang, C.; Yang, J.; Contreras, D. S.; Clancy, Y. L.; Lobkovsky, E. B.; Yaghi, O. M.; Dai, S. *Angew. Chem., Int. Ed.* **2006**, *45*, 1390.

(2) (a) Lee, J.; Li, J.; Jagiello, J. *J. Solid State Chem.* **2005**, *178*, 2527. (b) Sun, D.; Ke, Y.; Mattox, T. M.; Ooro, B. A.; Zhou, H.-C. *Chem. Commun.* **2005**, 5447. (c) Lin, X.; Jia, J.; Zhao, X.; Thomas, K. M.; Blake, A. J.; Walker, G. S.; Champness, N. R.; Hubberstey, P.; Schröder, M. *Angew. Chem., Int. Ed* **2006**, *45*, 7358. (d) Li, H.; Eddaoudi, M.; O'Keeffe, M.; Yaghi, O. M. *Nature* **1999**, *402*, 276.

(3) (a) Halder, G. J.; Kepert, C. J.; Moubaraki, B.; Murray, K. S.; Cashion, J. D. *Science* **2002**, *298*, 1762. (b) Cheng, X.-N.; Zhang, W.-X.; Lin, Y.-Y.; Zheng, Y.-Z.; Chen, X.-M. *Adv. Mater.* **2007**, *19*, 1494. (c) Zeng, M.-H.; Feng, X.-L.; Zhang, W.-X.; Chen, X.-M. *Dalton Trans.* **2006**, 5294.

(4) Alvaro, M.; Carbonell, E.; Ferrer, B.; Llabrés i Xamena, F. X.; Garcia, H. *Chem.−Eur. J.* **2007**, *13*, 5106.

(5) (a) Eddaoudi, M.; Moler, D. B.; Li, H.; Chen, B.; Reineke, T. M.; O'Keeffe, M.; Yaghi, O. M. *Acc. Chem. Res.* **2001**, *34*, 319. (b) Sun, D.; Ma, S.; Ke, Y.; Petersen, T. M.; Zhou, H.-C. *Chem. Commun.* **2005**, 2663. (c) Jia, J.; Lin, X.; Wilson, C.; Blake, A. J.; Champness, N. R.; Hubberstey, P.; Walker, G.; Cussen, E. J.; Schröder, M. *Chem. Commun.* **2007**, 840. (d) Dincă, M.; Han, W. S.; Liu, Y.; Dailly, A.; Brown, C. M.; Long, J. R. *Angew. Chem., Int. Ed.* **2007**, *46*, 1419. (e) Dincă, M.; Dailly, A.; Liu, Y.; Brown, C. M.; Neumann, D. A.; Long, J. R. *J. Am. Chem. Soc.* **2006**, *128*, 16874. (f) Fang, Q.-R.; Zhu, G.-S.; Jin, Z.; Xue, M.; Wei, X.; Wang, D.-J.; Qiu, S.-L. *Angew. Chem., Int. Ed.* **2006**, *45*, 6126.

(6) (a) Eddaoudi, M.; Kim, J.; Rosi, N.; Vodak, D.; Wachter, J.; O'Keeffe, M.; Yaghi, O. M. *Science* **2002**, *295*, 469. (b) Mueller, U.; Schubert, M.; Teich, F.; Puetter, H.; Schierle-Arndt, K.; Pastré, J. *J. Mater. Chem.* **2006**, *16*, 626.

(7) (a) Chun, H.; Dybtsev, D. N.; Kim, H.; Kim, K. *Chem.−Eur. J.* **2005**, *11*, 3521. (b) Chae, H. K.; Siberio-Pérez, D. Y.; Kim, J.; Go, Y.; Eddaoudi, M.; Matzger, A. J.; O'Keeffe, M.; Yaghi, O. M. *Nature* **2004**, *427*, 523. (c) Sun, D.; Collins, D. J.; Ke, Y.; Zuo, J.-L.; Zhou, H.-C. *Chem.−Eur. J.* **2006**, *12*, 3768.

10.1021/ic702085x CCC: $40.75
Published on Web 01/19/2008

Scheme 1. Structures of the bpz and bdc Ligands

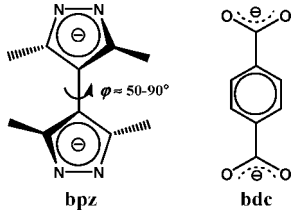

Ni(II), Cu(I) and Ag(I),[8] especially Cu(I) and Ag(I), furnishing triangular $[M_3(NN)_3]$ clusters.[8c,d] Such a tetradentate bridging mode is similar to that of 1,4-benzenedicarboxylate (bdc) in many known porous MOFs. Moreover, the two pyrazolate rings in bpz can rotate in the range of 50−90° to have potential flexibility for the resulting MOFs, and the presence of methyl groups on bpz ligand may be beneficial not only for preventing interpenetration of the MOFs but also for tuning the size and surface property of the pores. Therefore, bpz ligands can be expected to replace part of bdc ligands in linking the tetrahedral Zn_4O clusters into a mixed-ligand bridged MOF. Herein, we present a new three-dimensional (3D) MOF, $[Zn_4O(bdc)(bpz)_2]\cdot 4DMF\cdot 6H_2O$ (**1**), constructed from a Zn_4O cluster with bdc and bpz linkers, which exhibits nice guest sorption, as well as guest-dependent luminescent properties.

Experimental Section

Materials and General Methods. All solvent and starting materials for synthesis were purchased commercially and were used as received. Infrared spectra were obtained from KBr pellets on a Bruker TENSOR 27 Fourier transform infrared spectrometer in the 400–4000 cm^{-1} region. Elemental analysis (C, H, N) was performed on a Perkin-Elmer 240 elemental analyzer. Thermogravimetric analysis (TGA) was performed at a rate of 10 °C/min under N_2 using a NETZSCH TG 209 system. Powder X-ray diffraction (PXRD) data were recorded on a Rigaku D/M-2200T automated diffractometer. The solid samples for photoluminescent measurements were obtained through soaking the desolvated samples in benzene, toluene, and *p*-xylene for 15 h, respectively, and then dried for 15 h at room temperature. The same process was applied to the preparation of xylene- and 1,3,5-trimethylbenzene-adsorbed samples for TGA. The solid-state photoexcitation and emission spectra were performed on a RF-5301PC spectrophotometer at room temperature.

Synthesis of $[Zn_4O(bdc)(bpz)_2]\cdot 4DMF\cdot 6H_2O$ (1). A mixture of H_2bdc (0.025 g, 0.15 mmol), H_2bpz (0.057 g, 0.30 mmol), and $Zn(NO_3)_2\cdot 6H_2O$ (0.179 g, 0.60 mmol) in *N*,*N*′-dimethylformamide (DMF) (9 mL) was placed in a Teflon-lined stainless steel vessel (12 mL) and heated at 140 °C for 80 h, and then it was cooled to room temperature at a rate of 0.1 °C/min. The resulting white microcrystalline precipitate of **1** was isolated by ultrasonication (10 s) and decanting of the supernatant suspension, which was washed with DMF/ethanol and dried in vacuo. The yield was 88 mg (48%). Colorless single crystals for X-ray single-crystal diffraction were prepared by heating a solution of H_2bdc (0.025 g, 0.15 mmol), H_2bpz (0.029 g, 0.15 mmol), and $Zn(NO_3)_2\cdot 6H_2O$ (0.089 g, 0.30 mmol) in 9 mL of DMF in a 12 mL Teflon-lined stainless steel vessel at 120 °C for 80 h, and then the mixture was cooled to room temperature at a rate of 0.1 °C/min. The yield was ∼40 mg (22%). Anal. Calcd for $C_{40}H_{68}Zn_4N_{12}O_{15}$: C, 39.42; H, 5.62; N, 13.79. Found: C, 39.20; H, 5.56; N, 13.92%. IR (KBr, cm^{-1}): 3445m, 2924m, 1670vs, 1581s, 1503m, 1391s, 1256w, 1056m, 820w, 764m, 562w.

Table 1. Crystallographic Data and Structural Refinements for **1**

formula	$C_{40}H_{68}Zn_4N_{12}O_{15}$
fw (g/mol)	1218.54
T (K)	293(2)
cryst syst	tetragonal
space group	$P4_2/mcm$
a (Å)	11.5228(4)
c (Å)	25.7692(19)
V (Å^3)	3421.5(3)
Z	2
D_c (g cm^{-3})	1.183
μ (mm^{-1})	1.442
reflns collected/uniqe (R_{int})	12617/1833 (0.0358)
R1[a] (>2σ/all data)	0.0496/0.0566
wR2[b] (>2σ/all data)	0.1442/0.1492
GOF	1.114

[a] $R1 = \sum F_o| - |F_c/\sum|F_o|$. [b] $wR2 = [\sum w(F_o^2 - F_c^2)^2/\sum w(F_o^2)^2]^{1/2}$.

Table 2. Selected Bond Lengths (Å) and Angles (deg) for **1**[a]

Zn1−N1	1.981(3)	Zn1−O1	1.970(4)
Zn1−N1$^{\#1}$	1.981(3)	Zn1−O2	1.9400(5)
N(1)−Zn(1)−N(1)$^{\#1}$	123.1(2)	O(1)−Zn(1)−O(2)	109.6(1)
N(1)−Zn(1)−O(2)	99.28(9)	N(1)−Zn(1)−O(1)	111.6(1)

[a] Symmetry code: #1 *y*, *x*, *z*.

Sorption Measurements. The sorption isotherm for N_2 gas was measured with an automatic volumetric adsorption apparatus (Micrometrics ASAP 2010) at 77 K, and the sorption isotherms for methanol, benzene, and toluene vapors were measured with an automatic gravimetric adsorption apparatus (IGA-003 series, Hiden Isochema Ltd.) at 298 K. The as-synthesized samples (weight 165 mg) were placed in a quartz tube and dried under high vacuum at 393 K for 12 h to remove the solvated molecules prior to measurements. The BET surface area was calculated from a line regression plot of $1/(W((P_0/P) - 1))$ versus P/P_0 (where W is the total volume absorbed at particular P/P_0 point and P_0 is 1 atm pressure) within the range of $0.02 < P/P_0 < 0.25$.

Crystallography. The diffraction data were collected at 293(2) K with a Bruker AXS SMART CCD area detector diffractometer using ω -rotation scans with a scan width of 0.3° and Mo Kα radiation (λ = 0.71073 Å). Absorption corrections were carried out using SADABS.[9] The structure was solved by the direct methods and refined by full-matrix least-squares refinements based on F^2.[10] All nonhydrogen atoms except for disordered solvent molecules were refined anisotropically, with the hydrogen atoms added to their geometrically ideal positions and refined isotropically. Disordered DMF and water molecules were located from the difference Fourier maps, and DFIX was used to refine DMF. The formula was determined by combining single-crystal structure, elemental microanalysis, and TGA. Selected bond lengths and angles were given in Table 2.

Results and Discussion

Synthesis and Structural Characterization. Many examples have proven that amides, such as DMF, DEF

(8) (a) Kruger, P. E.; Moubaraki, B.; Fallon, G. D.; Murray, K. S. *J. Chem. Soc., Dalton Trans.* **2000**, 713. (b) Kruger, P. E.; Fallon, G. D.; Moubaraki, B.; Murray, K. S. *J. Chem. Soc., Chem. Commun.* **1992**, 1726. (c) Zhang, J.-P.; Horike, S.; Kitagawa, S. *Angew. Chem., Int. Ed.* **2007**, *46*, 889. (d) He, J.; Yin, Y.-G.; Wu, T.; Li, D.; Huang, X.-C. *Chem. Commun.* **2006**, 2845.

(9) *SADABS*, *SMART*, and *SAINT*. Bruker AXS Inc.: Madison, WI, 2002.

(10) Sheldrick, G. M. *SHELXL-97, Program for the Refinement of Crystal Structures*; University of Göttingen: Göttingen, Germany, 1997.

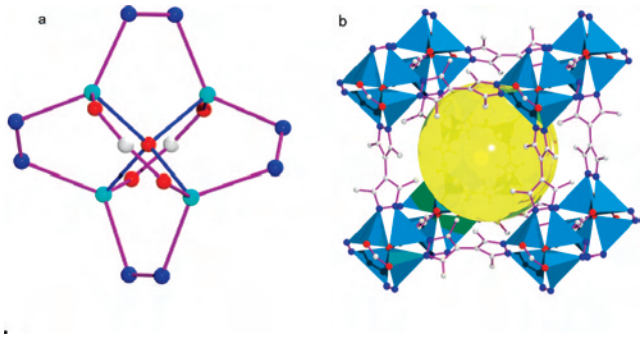

Figure 1. (a) Ball-and-stick representation of the $Zn_4O(CO_2)_2(NN)_4$ SBU in **1**. (b) Cubelike cavity within **1** formed by eight tetranuclear clusters (Zn, cyan; N, blue; O, red; C, white).

(*N*,*N*′-diethylformamide), and DMA (*N*,*N*′-dimethylacetamide), can provide an efficient environment for the formation of many types of metal carboxylate MOFs. Similarly, colorless, cubelike single crystals of **1** suitable for structural study were prepared by a solvothermal reaction of H_2bdc, H_2bpz, and $Zn(NO_3)_2$ with a molar ratio of 1:1:2 in DMF at 120 °C for 80 h. However, X-ray diffraction (PXRD) patterns revealed impurity of the bulk samples. The phase-pure bulk samples verified by PXRD were obtained with a molar ratio 1:2:4, for bdc, bpz, and $Zn(NO_3)_2$ at 140 °C for 60 h and were subsequent carefully treated. Compound **1** is insoluble in water and common organic solvents and becomes opaque in the air.

It is also worth noting that after many trials via changing the zinc salts, solvent, and temperature, we failed to obtain a $Zn_4O(bpz)_6$-based MOF in the absence of carboxylate coligand. Presumably, the participation of two less bulky carboxylate groups is helpful in stabilization of the Zn_4O core in **1**.

Single-crystal structure analysis reveals that **1** crystallizes in the tetragonal space group $P4_2/mcm$, and exhibits a 3D framework built from μ_4-oxo-centered tetranuclear Zn_4O clusters with bdc and bpz linkers. In **1**, each Zn(II) atom adopts a tetrahedral coordination environment with two nitrogen atoms from different pyrazolate rings [Zn−N = 1.981(3) Å], one carboxylate oxygen atom [Zn−O = 1.970(4) Å], and one μ_4-oxo atom [Zn−O = 1.9400(5) Å] (Figure 1). Thus, each Zn_4O cluster forms an octahedral $Zn_4O(CO_2)_2(NN)_4$ SBU through edge-bridging coordination of four pyrazolate and two carboxylate groups (Figure 1). To our knowledge, no such $Zn_4O(CO_2)_2(NN)_4$ SBU has been reported in the literature. In addition, compared with those well-known trinuclear $[M_3(NN)_3]$ [M = Cu(I) or Ag(I)] motifs based on bpz,[8c,d] tetranuclear clusters constructed by bpz have not been reported previously. Each Zn_4O cluster connects four bpz, and each bpz binds two clusters into a 4^4 2D layer parallel to the *ab* plane. The layers are further pillared along the *c*-axis by bdc ligands to form a neutral, noninterpenetrated 3D porous network with a six-connected CaB_6 topology (Figure 2). The distances of the adjacent Zn_4O centers in **1** separated by bdc and bpz ligands are 12.9 and 11.5 Å, respectively, and a cubelike cavity is surrounded by eight Zn_4O clusters with the dimensions of 12.9 × 11.5 × 11.5 Å^3, in which four DMF and six water guest molecules

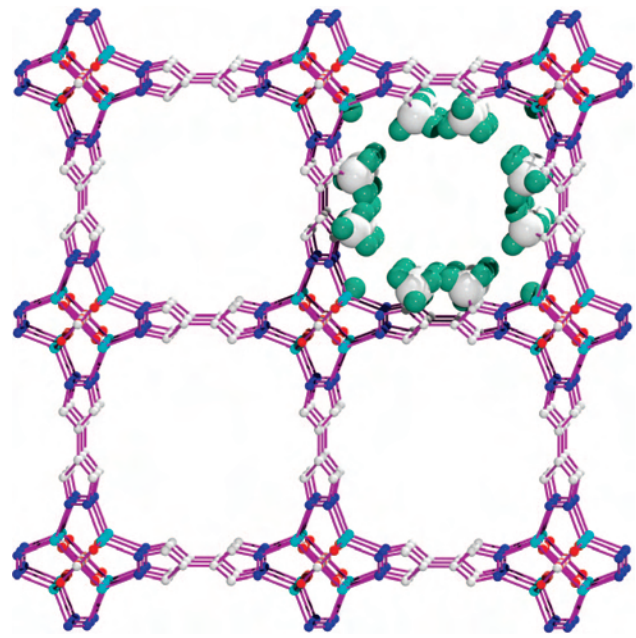

Figure 2. 3D porous network of **1** viewed along the *c*-axis with the methyl groups are highlighted in one channel.

reside (Figure 1). The two pyrazolate rings of bpz are tilted with an angle of 79.5°, while the four methyl groups from four different bpz ligands direct inward each cavity, thus narrowing window sizes in **1**, which are 4.9 × 6.8 Å^2 and 5.7 × 5.7 Å^2 (excluding van der Waals radii) along the *a*- (or *b*-) and *c*-axes, respectively, being smaller than that in $[Zn_4O(bdc)_6]$ (MOF-5, 8.0 × 8.0 Å^2).[2d] The methyl groups in **1** define a hydrophobic cavity, and the nearest guest–host distance of 4.157 Å is from the lattice-water molecule O2w and aryl C6, precluding any significant guest–host hydrogen bonding. The solvent accessible volume of **1** is estimated by PLATON[11] to be 63.3% of the total crystal volume. Rationally, the existence of methyl groups of bpz ligand and the formation of Zn_4O cluster contribute to the formation of noninterpenetrated network of **1**.

TGA and PXRD. The thermal stability of **1** was examined by TGA and PXRD patterns. The PXRD pattern of the as-synthesized sample is uniform to that simulated from the single-crystal structure, showing the phase purity of the bulk samples (Figure 3). Under a dinitrogen atmosphere, TGA reveals a weight loss of 31.5% from 30 to 225 °C, corresponding to six waters and four DMF solvates (calcd 32.8%), and no further weight loss from 225 to 390 °C (Figure S1). Upon further heating, the obvious weight loss above 390 °C corresponds to the decomposition of **1**. At 600 °C, the overall weight loss of 48.5% for **1** indicates an incomplete decomposition and the presence of ligand and nitride residue.

The guest molecules in **1** can be easily removed by exchange with CH_2Cl_2 for 48 h and subsequent heating at 100 °C under vacuum for 5 h, which can be verified by TGA on the desolvated **1**. The fully desolvated **1** exhibits no obvious weight loss from 30 to 390 °C (Figure S1). Meanwhile, the lack of the C=O stretching peak at 1670

(11) Spek, A. L. *J. Appl. Crystallogr.* **2003**, *36*, 7.

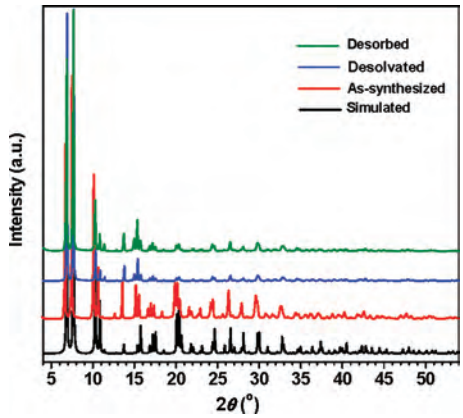

Figure 3. PXRD patterns of **1** simulated from the X-ray single-crystal structure, as-synthesized, desolvated, and benzene-desorbed samples of **1**.

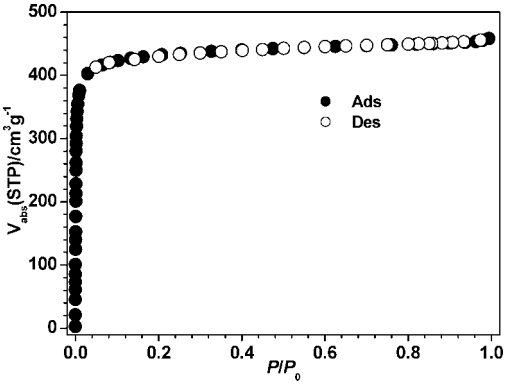

Figure 4. Nitrogen sorption isotherm of **1** at 77 K (P_0 = 1 atm).

cm^{-1} in the IR spectrum of desolvated **1** (Figure S2) also confirms the full release of DMF guests. The PXRD pattern of desolvated **1** is approximately identical to that of the as-synthesized sample, indicating the architectural hold after evacuation.

Sorption Properties. To examine the pore characteristics and storage capability, the sorption properties of the desolvated **1** have been performed with N_2 gas and different volatile organic molecules.

The N_2 sorption measurements of desolvated **1** at 77 K indicate a reversible type-I isotherm (Figure 4), characteristic of microporous material. The Langmuir surface area is fitted to be 1908 m^2/g (BET surface area, 1476 m^2/g), which is inferior to that of MOF-5 (2900 m^2/g)[2d] but much higher than the highest value for zeolites, zeolite Y (904 m^2/g),[12] and comparable to those of active carbon (Ceca, carbon AC40, 2000 m^2/g) and [$Zn_4O(ndc)_6$] (ndc = 2,6-naphthalenedicarboxylate) or IRMOF-8 (1750 m^2/g).[6b] Such a porous material with a surface area of ~2000 m^2/g, a void of ~60%, and free windows of ~6 Å, has promising storage capacity.[7a] The N_2 uptake of 459 cm^3/g (STP) (573 mg/g) of **1** is obtained at 1 atm, which corresponds to 16.7 molecules per formula unit or one cavity (see Figure 1) and comparable to those of some MOFs, such as [$Cu_2(L)(H_2O)$][2c] [L = biphenyl-3,3′,5,5′-tetracarboxylate, 448 cm^3/g (STP)] and [Zn_2(bdc)(dabco)] [475 cm^3/g (STP)],[7a] having similar

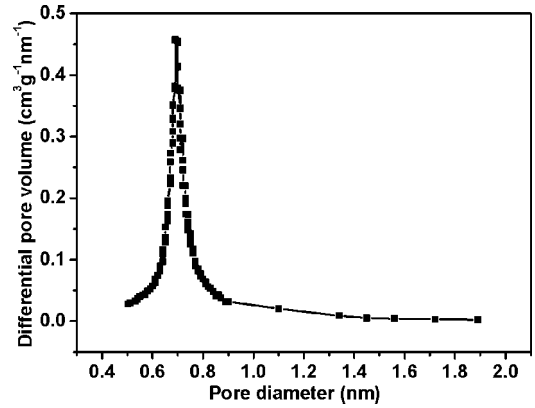

Figure 5. Micropore size distribution of **1**.

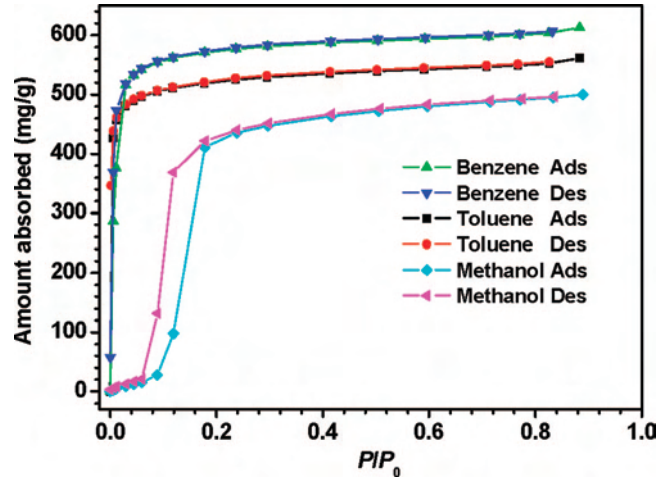

Figure 6. Methanol, benzene, and toluene sorption isotherms of **1** at 298 K. P_0 is respective saturated vapor pressure.

specific surface areas and solvent-accessible volumes. The Horvath–Kawazoe (HK) model[13] indicates a pore diameter of ~6.9 Å for **1**, as shown in Figure 5, consistent with the X-ray analysis. Using the t-plot model, the micropore volume is 0.58 cm^3/g.

The high porosity of **1** allows potential access by a variety of small solvent molecules. The sorption behaviors of methanol, benzene, and toluene at 298 K also feature a typical type-I isotherm, as shown in Figure 6. At P/P_0 = 0.10, the adsorptions of benzene and toluene reach saturation, indicating strong guest–host interactions; the amount adsorbed for benzene and toluene are 561 and 510 mg/g or 5.9 and 4.5 molecules per formula unit, respectively, inferior to MOF-5 (802 mg/g for benzene at 295 K),[5a] but superior to other MOF materials.[14] For some reported benzene-adsorbed MOFs, discernible hysteresis was observed because of guest–host C−H···π or π···π interactions.[14a,c] However, no hysteresis is found upon desorption of benzene on **1**, indicating that incoming guests can move freely into and out of the pores, which results from the smaller dimensions

(12) Chester, A. W.; Clement, P.; Han, S. U.S. Patent Appl. 2000/6136291A, 2006.

(13) Horvath, G.; Kawazoe, K. *J. Chem. Eng. Jpn.* **1983**, *16*, 470.

(14) (a) Lin, X.; Blake, A. J.; Wilson, C.; Sun, X. Z.; Champness, N. R.; George, M. W.; Hubberstey, P.; Mokaya, R.; Schröder, M. *J. Am. Chem. Soc.* **2006**, *128*, 10745. (b) Eddaoudi, M.; Li, H.; Yaghi, O. M. J. *Am. Chem. Soc.* **2000**, *122*, 1391. (c) Xue, D.-X.; Lin, Y.-Y.; Cheng, X.-N.; Chen, X.-M. *Cryst. Growth Des.* **2007**, *7*, 1332.

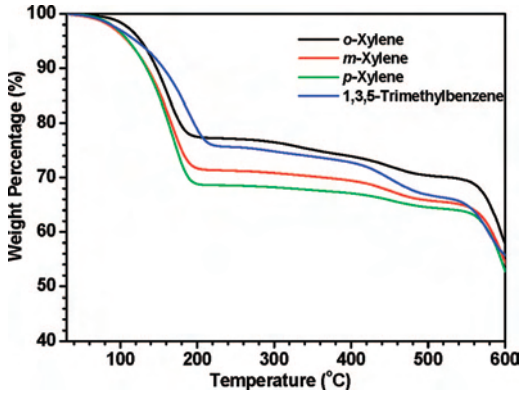

Figure 7. TGA plots of the *o*-, *m*-, and *p*-xylene and 1,3,5-trimethylbenzene adsorbed **1**.

of the benzene and toluene, 3.3 × 6.6 and 4.0 × 6.6 Å^2,[15] respectively, than the window sizes of the cavity. In contrast, the adsorption of methanol reveals an interesting two-step behavior with a small hysteresis. In the $P/P_0 < 0.08$ region, the loading is less than 25 mg/g, which is attributed to the incompatibility between the hydrophobic methyl antennas of the cavity and hydrophilic methanol molecules. At a P/P_0 value above 0.08, a steep increase in adsorption is from the capillary condensation filling the pores with methanol, similar to those observed in few MOF materials.[16] At $P/P_0 = 0.20$, a loading of 420 mg/g (10.7 molecules per formula unit) is available. The desorption hysteresis implies that possible weak guest–host hydrogen-bonding interactions might exist under relatively higher pressure. In addition, after desorption of the guest benzene molecules, the PXRD pattern reflects the structural intactness of the desorbed **1** (Figure 3).

According to the Dubinin–Radushkevich (DR) equation, the isosteric heat of adsorption, $q_{st,\Phi=1/e}$, can be estimated to be 12.5, 48.2, 56.9, and 64.8 kJ/mol for N_2, methanol, benzene, and toluene, respectively, which are comparable to those for active carbon and some MOFs.[14a,17]

The control of pore size is crucial for molecular storage and selective separation. Because the diagonal sizes of the windows in **1** are 8.1 and 8.4 Å along the *c*-and *a*- (or *b*-) axes, respectively, *o*-, *m*-, and *p*-xylene and 1,3,5-trimethylbenzene guests with respective sizes of 3.8 × 7.3, 3.9 × 7.3, 3.8 × 6.6, and 4.1 × 8.2 Å^2 [15] were chosen for probing. TGA measurements indicate weight losses of 22.5, 28.0, and 31.2% for xylene within 200 °C corresponding to 2.3 *o*-xylene, 3.0 *m*-xylene, and 3.5 *p*-xylene molecules per formula unit, respectively, as shown in Figure 7. The weight loss of 23.8% before 220 °C for 1,3,5-trimethylbenzene equals 2.1 molecules. The sorption amount depends on molecular sizes and geometry. Thus a free-passage of ~8.2 Å is available for **1**. Moreover, comparison of the PXRD patterns of xylene-adsorbed samples with that of **1** reveals no significant structure change (Figure S9), which is very

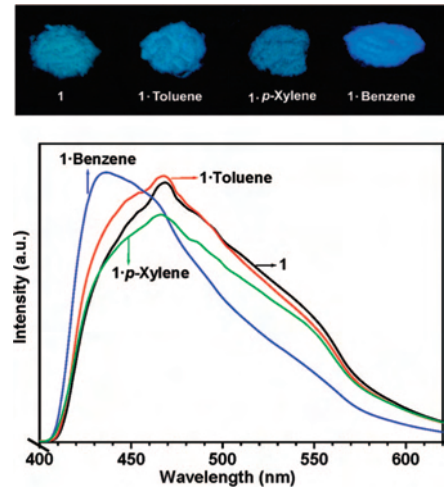

Figure 8. (Top) Snapshot of the as-synthesized, benzene-, toluene-, and *p*-xylene-adsorbed samples of **1** under UV irradiation, showing stronger luminescence for benzene-adsorbed **1**. (Bottom) Emission spectra of the above four samples in solid state with excitation at 355 nm.

important for repeating application of the storage materials. These findings imply that **1** may be used for size-selective separation with a critical molecule size of ~8.2 Å.

Luminescent Properties. Upon excitation at 355 nm, solid **1** exhibits extensive blue luminescence centered at λ_{max} = 470 nm (Figure 8). Since similar emissions with λ_{max} at 474 and 418 nm were also observed for H_2bpz (Figure S11) and Na_2bdc[18] in solid state, respectively. The photoluminescence of **1** may be tentatively assigned to the intraligand fluorescent emissions. In addition, several Zn-MOFs have shown interesting guest-dependent, such as organic solvents and lanthanide ions, luminescent properties,[19] thus exhibiting potential application in luminescent sensors. The nice sorption capacity of **1** encourages us to characterize the possible guest-dependent luminescent behavior. Interestingly, blue shifts are observed for benzene-, toluene-, and *p*-xylene-adsorbed samples of **1**, with λ_{max} at 435, 465, and 466 nm, respectively, upon excitation at 355 nm in solid state. Notably, because a structurally similar MOF of **1**, MOF-5 was proven to be elastic and not rigid at room temperature,[20] it can be expected that the framework of **1** is also elastic, even more than MOF-5, because of the vibration of methyl groups. Consequently, the above luminescent phenomenon can be rationally attributed to the structural reinforcement upon the inclusion of rigid guest molecules, which weaken skeletal vibration, stabilize the framework and enhance the intraligand $\pi-\pi^*$ energy. Thus, a stronger and higher energy emission is found. Especially for benzene-treated **1**, the markedly stronger and blue-shifted emission results from more adsorbed amount of benzene compared with those of toluene and *p*-xylene in **1**, since the more sorption may

(15) Webster, C. E.; Drago, R. S.; Zerner, M. C. *J. Am. Chem. Soc.* **1998**, *120*, 5509.
(16) (a) Huang, X.-C.; Lin, Y.-Y.; Zhang, J.-P.; Chen, X.-M. *Angew. Chem., Int. Ed.* **2006**, *45*, 1557. (b) Pan, L.; Parker, B.; Huang, X.; Olson, D. H.; Lee, J.; Li, J. *J. Am. Chem. Soc.* **2006**, *128*, 4180.
(17) Ramirez, D.; Qi, S.; Rood, M. J. *Environ. Sci. Technol.* **2005**, *39*, 5864.
(18) Bordiga, S.; Lamberti, C.; Ricchiardi, G.; Regli, L.; Bonino, F.; Damin, A.; Lillerud, K.-P.; Bjorgen, M.; Zecchina, A. *Chem. Commun.* **2004**, 2300.
(19) (a) Sun, S.-S.; Lees, A. J. *Coord. Chem. Rev.* **2002**, *230*, 171. (b) Lee, E. Y.; Jang, S. Y.; Suh, M. P. *J. Am. Chem. Soc.* **2005**, *127*, 6374. (c) Sun, D.; Ke, Y.; Collins, D. J.; Lorigan, G. A.; Zhou, H.-C. *Inorg. Chem.* **2007**, *46*, 2725.
(20) Mattesini, M.; Soler, J. M.; Ynduráin, F. *Phys. Rev. B* **2006**, *73*, 094111.

induce the less vibration of the framework for the marked luminescent change. Similar luminescent blue shifts, with increasing the amount of solvent molecules, have also been revealed for other MOFs.[21] These results imply that **1** may be applied in luminescent detection for benzene molecules from its derivatives.

Conclusions

In summary, we have prepared a new 3D porous MOF based on Zn_4O clusters incorporating bdc and bpz ligands, which features methyl groups on the pore surface and hydrophobic properties. Compound **1** exhibits high porosity, high adsorption capacity for gas and organic solvent molecules, and guest-dependent luminescent properties, which may serve as a promising candidate for applications as molecular separation and storage materials, as well as selective luminescent detection for benzene.

Acknowledgment. This work was supported by NSFC (No. 20531070), the "973 Project" (2007CB815302), and Science and Technology Department of Guangdong Province (No. 04205405).

Supporting Information Available: PXRD, IR spectra, BET plot, Langmuir plot, DR plot, the excitation spectrum of **1**, emission spectrum of H_2bpz, and a CIF file. This material is available free of charge via the Internet at http://pubs.acs.org.

IC702085X

(21) Huang, Y.-Q.; Ding, B.; Song, H.-B.; Zhao, B.; Ren, P.; Cheng, P.; Wang, H.-G.; Liao, D.-Z.; Yan, S.-P. *Chem. Commun.* **2006**, 4906.